Single-particle configurations of low- and medium-spin states in math xmlns="http://www.w3.org/1998/Math/MathML">mmultiscripts>mi>Cu/mi>mprescripts>/mprescripts>none>/none>mn>63/mn>/mmultiscripts>/math>

S. Chatterjee, B. Mondal, S. Samanta, S. Das, R. Raut, S. S. Ghugre, P. C. Srivastava, A. K. Sinha, U. Garg, Neelam, Naveen Kumar, P. Jones, Md. S. R. Laskar, F. S. Babra, S. Biswas, S. Saha, P. Singh, and R. Palit

Single Particle Configurations of Low and Medium Spin States in ^{63}Cu

S. Chatterjee, B. Mondal, S. Samanta, S. Das, R. Raut,* and S. S. Ghugre
UGC-DAE Consortium for Scientific Research, Kolkata Centre, Kolkata 700098, India

P. C. Srivastava
Department of Physics, Indian Institute of Technology, Roorkee, Roorkee 247667, India

A. K. Sinha†
UGC-DAE Consortium for Scientific Research, University Campus, Khandwa Road, Indore 452017, India

U. Garg
Department of Physics and Astronomy, University of Notre Dame, Notre Dame, Indiana 46556

Neelam
Department of Physics and Astrophysics, University of Delhi, New Delhi 110007, India

Naveen Kumar
Government College, Haripur (Guler), District Kangra, Himachal Pradesh 176028, India

P. Jones
Department of Subatomic Physics, iThemba LABS, Somerset West 7129, South Africa

Md. S. R. Laskar, F. S. Babra, S. Biswas, S. Saha, P. Singh, and R. Palit
Tata Institute of Fundamental Research, Mumbai 400005, India
(Dated: January 24, 2023)

The excitation scheme of the ^{63}Cu nucleus has been probed following its population in a light-ion induced fusion-evaporation reaction and using an array of Compton suppressed HPGe clover detectors as the detection system. Apart from ascribing gamma-ray transitions to the level scheme of the nucleus, through γ-γ coincidence measurements, and identifying the new transitions in the process, measurements of angular correlation and linear polarization of the gamma-rays have also been carried out towards assigning their multipolarities and electric and magnetic character. The observed level scheme has been interpreted through shell model calculations in two different model spaces. One of these was the $f5pg9$ space outside the ^{56}Ni core while the other included $f_{7/2}$ orbital for the protons outside the ^{48}Ca core and was directed at probing the influence of the $f_{7/2}$ excitations in the regime of spins being investigated. The latter has been found to be of rather modest impact, in general, and the observed level structure can largely be interpreted through particle excitations in the $f5pg9$ model space.

PACS numbers: 23.20.Lv,21.10.Hw,21.60.Cs

I. INTRODUCTION

The Shell Model (SM) of the nucleus, even after several decades since its inception, continues to be of cardinal importance in our understanding of nuclear excitations. The preeminence of SM goes beyond its use in the interpretation of observed level structures, into facilitating an index for the acceptability of other models as well [1]. The limitations on the use of SM away from the shell closures, with increased number of valence nucleons and larger model space, are ascribed to the considerations of computational feasibility while the model itself remains one of the principal microscopic models for wide applications across the nuclear chart. There are continuous endeavors to counter the computational challenges and new effective interactions as well as truncation schemes are being developed in the process. Such developments are known to proceed through stringent comparison of model predictions with the available experimental data. The quality of representation of the data accomplished from a proposed interaction is indicative of its credibility and any such effort is typically based on fitting experimental observables with the corresponding calculations, over a wide range of relevant isotopes (for example, [2]). It is amply evidenced that experimental data, particularly on nuclei around the shell closures, provide for the wherewithal to validate shell model interactions and is

*Corresponding Author: rajarshi.raut@gmail.com
†Presently: Hon. Adjunct Professor, Department of Physics, Savitribai Phule Pune University, Pune, India

thus of pertinence in the progress of the model towards more efficient use.

The shell closure at $N, Z = 28$ is interesting in the context of aforementioned pursuits. It is the lowest magic number that emerge from the spin-orbit $(\vec{l}.\vec{s})$ coupling. Excitation schemes of nuclei with few valence nucleons outside the doubly-magic ^{56}Ni ($Z, N = 28$) core exhibit myriad structural features. While it is approximately valid to interpret the low and medium spin levels in these nuclei through single particle excitations in the $p_{3/2}$, $f_{5/2}$ and $p_{1/2}$ orbitals, there are observations that indicate $(f_{7/2})$ proton excitations across the $Z = 28$ shell gap assume significance therein [3]. The softness of the ^{56}Ni core is thus evidenced and that go a long way in impacting the level structure of the nuclei in discussion. At higher excitations, neutron occupancy of the intruder $g_{9/2}$ orbital constitute the single particle configurations and deformation driving effect of the same may consequent into observation of rotational sequences [4]. Neutron occupancy of the $g_{9/2}$ orbital may also need to be invoked in order to interpret the (near) ground state properties of neutron-rich isotopes in the vicinity of the ^{56}Ni core [3]. It is thus understood that a shell model approach towards interpreting the single particle excitations in nuclei around the ^{56}Ni core should be ideally based on the fpg model space consisting of $f_{7/2}$, $p_{3/2}$, $f_{5/2}$, $p_{1/2}$ and $g_{9/2}$ orbitals. The large dimensions (of the matrix for diagonalization) incurred in the process may present a computational hurdle. The issue is circumvented through effective interactions that incorporate only a restricted model space of $f_{5/2}pg_{9/2}$ orbitals, while approximating the influence of the $f_{7/2}$ orbital through the interactions of these active ones. The results therefrom are of varying compliance with those obtained from measurements. Two such interactions widely used in this context are $JUN45$ [5] and $jj44bpn$ [6]. Notwithstanding their success in identifying the excitations that constitute the level structure of nuclei with valence nucleons outside the ^{56}Ni core, they are still short of producing a comprehensive computation. The pfg_{9a} [7, 8] interaction, on the other hand, includes the entire fpg basis while allowing excitations from the $f_{7/2}$ orbital and excitations into the $g_{9/2}$ orbital and is thus expected to facilitate a detailed insight of the single particle configurations for these nuclei. Advances in the computing viability, as have been accomplished in the recent years, cater to the befitting framework for such large basis shell model calculations.

The isotopes of Ni ($Z = 28$) and Cu ($Z = 29$), with few nucleons outside the $Z, N = 28$ closure, have been of pertinence in probing the aforementioned interactions. There have been recent efforts [3, 9–11] directed at constructing the level schemes of these nuclei, using state-of-the-art experimental setups, followed by shell model calculations, using different interactions, aimed at faithful reproduction of the measurements. The particle

configurations that constitute the excitation schemes get identified in the process. The ^{63}Cu ($Z = 29, N = 34$) is one such system that has been investigated in several studies through evolving detection facilities and advances in shell model calculations, as enlisted in the compilation of Ref. [12]. Some of these studies, such as that by Mukherjee et $al.$ [13], and a later investigation by Rai et $al.$ [14], were based on the population of the nucleus, in its excited states, through heavy-ion induced fusion-evaporation reactions and used high-resolution, efficient HPGe detector arrays that befitted the spectroscopy objectives. Mukherjee et $al.$ [13] had ascribed the states, upto excitation energy $E_x \approx 7$ MeV and spin $\approx 11\hbar$, to particle configurations in the restricted basis consisting of $f_{5/2}, p_{3/2}, p_{1/2}, g_{9/2}$ orbitals while noting that the excitations from $f_{7/2}$ orbital might be of importance. The interaction used was that by Koops and Glaudemans [15]. Rai et $al.$ [14] has recently reported an updated level scheme of the nucleus while using a larger array of HPGe (clover) detectors as the detection system. The level scheme of ^{63}Cu, as proposed by Rai et $al.$, is extended upto $E_x \approx 9.5$ MeV and spin $\approx 12\hbar$ and has been represented through particle excitations in the same $f_{5/2}pg_{9/2}$ ($f5pg9$) space, albeit with more contemporary JUN45 [5] and jj44b (Ref. 59 of Rai et $al.$) interactions. The overlap of the calculated level energies with the experimental ones was found to be differing for the two interactions used, with the jj44b leading to better compliance with respect to that produced by JUN45.

This paper reports a reinvestigation of the excitations in ^{63}Cu nucleus following its production in a light-ion induced fusion-evaporation reaction that is expected to favorably populate the non-yrast states of the level structure. The level energies have been calculated in both the $f5pg9$ as well as the $fpg9$ basis in order to estimate the impact of particle excitations from the $f_{7/2}$ orbital. Chiara et $al.$ [3] has observed that the latter is necessary to appropriately represent the observed excitation schemes of Cu isotopes with $A \leq 63$ and one of the objectives of the present work has been to explore the proposition.

II. EXPERIMENTAL DETAILS AND DATA ANALYSIS

The ^{63}Cu nucleus was produced in the ^{59}Co(^{7}Li,$p2n$) reaction at E_{lab} = 22-24 MeV. The ^{7}Li beam was delivered by the 14 UD Pelletron at the Pelletron LINAC Facility in TIFR, Mumbai. The target consisted of 5.2 mg/cm^2 of ^{59}Co, that is mono-isotopic, evaporated onto a Ta backing of 4 mg/cm^2. An array of 10 Compton suppressed HPGe clover detectors was used as the detection system. The detectors were distributed at angles 90° (4 detectors), 115° (1 detector), 140° (3 detectors) and 157° (2 detectors). However, the two detectors at

157° had three (out of four) crystals working in each of them. Energy dependent efficiency of the detector array, and that of the individual sets of detectors at different angles, was determined using standard radioactive sources at the target position. Each detector of the array was at distance 25 cm from the target position [16]. The absolute (full-energy peak) efficiency of the detector array, at 1.33 MeV, was around 1.6% while that of the individual rings of detectors were around 0.6%, 0.2%, 0.5%, and 0.3% respectively for 90°, 115°, 140° and 157°. List mode data were acquired using a digitizer based system wherein the principal hardware was 12-bit 100 MHz PIXIE-16 digitizer modules manufactured by XIA LLC, USA [16]. The data was acquired under the condition of coincidence multiplicity of at least two detectors. The time window for coincidence was set to 100 ns. The event rate was $\approx$ 6 kcps, on the average, and around 10^9 two- and higher-fold events were recorded in the experiment.

The $p2n$ channel of the fusion-evaporation reaction, that was used to populate the excited states in ^{63}Cu, was not one with substantial cross section. Its yield was $\approx$ 45% of the $2n$ channel, that led to the production of ^{64}Zn, and that was the most dominant product. Spectroscopic investigations on other nuclei populated in the same reaction have been previously reported [10, 11] as a part of our continuing programme on the study of single particle excitations in nuclei in the vicinity of the ^{56}Ni core. The data analysis procedures applied in this work are largely in overlap with those pursued in the earlier papers. The MARCOS [16] code was used to construct symmetric and angle-dependent $\gamma - \gamma$ matrices that were analyzed using the RADWARE [17] package in order to extract the typical spectroscopic information of interest. The latter include energy, intensity and coincidence relationships of γ-ray transitions, their multipolarity and their electric and magnetic character, which are used to extract the energies and spin-parities of the levels that make up the excitation scheme.

The multipolarities of γ-ray transitions have been determined from the Ratio of Angular Distribution from Oriented (R_{ADO}) nuclei defined, for a γ-ray transition (γ_1), through [10, 11],

$$R_{ADO} = \frac{I_{\gamma 1}\ at\ 140^o\ (Gated\ by\ \gamma_2\ at\ all\ angles)}{I_{\gamma 1}\ at\ 115^o\ (Gated\ by\ \gamma_2\ at\ all\ angles)} \quad (1)$$

wherein I denotes the intensity of the transition, as determined through appropriate gate on the angle dependent asymmetric matrices that were constructed for the purpose. The reference values of R_{ADO}, for pure dipole and quadrupole transitions, are identical to the ones quoted in our earlier papers and have been determined from the weighted average of the number obtained for transitions belonging to other nuclei populated in the same reaction. These are 0.81(1) for stretched (ΔJ =
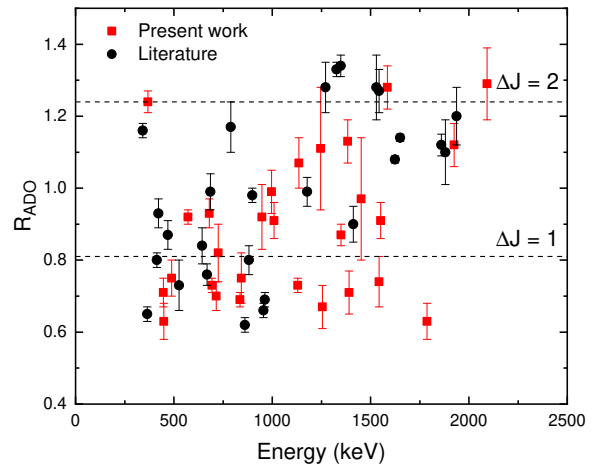

FIG. 1: R_{ADO} values for different transitions of ^{63}Cu. The reference values for the pure dipole and the pure quadrupole transitions are adopted from Samanta *et al.* [10, 11] and have been determined from the weighted average of R_{ADO} values for transitions in other nuclei produced in the same measurement. The transitions for which multipolarity have been newly assigned or have been modified from the previous assignment, following this work, are marked in red while transitions for which multipolarity were known previously (and have been confirmed in this study) are marked in black. Not all of the previously known transitions have been included in this plot. All the R_{ADO} values, however, are recorded in Table I.

1) pure dipole and 1.24(2) for stretched (ΔJ = 2) pure quadrupole transitions. R_{ADO} values between these limits indicate mixed transitions, predominantly dipole and quadrupole. The R_{ADO} values for the transitions in ^{63}Cu, as resulting from the present analysis, have been plotted in Fig. 1.

The linear polarization of γ-ray transitions, that indicate their electric and magnetic nature, are extracted from the scattering asymmetry between the planes perpendicular to and parallel to the reaction plane. The measurement is facilitated by the use of clover detector, with four crystals in one cryostat, wherein each crystal can operate as a scatterer and the adjacent ones as absorbers. The details of the exercise can be found in several references including our previous papers [10, 11] and we present only a brief summary of the same here. The asymmetry is represented through,

$$\Delta = \frac{aN_\perp\ -\ N_\parallel}{aN_\perp\ +\ N_\parallel} \quad (2)$$

wherein $N_\perp$ and $N_\parallel$ are the number of scattered photons, of a given γ-ray, that are scattered perpendicular to and parallel to the reaction plane, respectively. These

are extracted from the respective asymmetric matrices, as detailed elsewhere [10, 11]. The parameter a is the inherent geometrical asymmetry of the detection system and is estimated from the measure of asymmetry between the parallel and perpendicular scattering of γ-rays from an unpolarized radioactive source for which, ideally, $N_\parallel = N_\perp$ but, actually, is $N_\parallel = aN_\perp$. The value of a used in the present analysis is adopted from our earlier works [10, 11], carried out using the same setup, and is 1.017(4). The Δ values of transitions in ^{63}Cu, as determined in this analysis, are plotted in Fig. 2. The measurement of polarization asymmetry (Δ) is dependent on the difference of Compton scattering probability in the planes that are parallel to and perpendicular to the reaction plane. It is understood that the probability of Compton scattering interaction itself is a function of γ-ray energy and so is the difference between $N_\perp$ and $N_\parallel$. The energy dependence can be eliminated by normalizing the asymmetry Δ with the energy dependent polarization sensitivity (Q) and thus quoting the polarization as,

$$P = \frac{\Delta}{Q} \tag{3}$$

As has been detailed elsewhere [10, 11], Q is determined from the experimental Δ and the theoretical P, as calculated using the method in Ref. [18], of known transitions that are either pure or of known mixing. The Q values for such transitions are plotted as a function of their energies, preferably distributed over the range observed in the experiment, and fitted using,

$$Q(E_\gamma) = Q_0(E_\gamma)(CE_\gamma + D) \tag{4}$$

with,

$$Q_0(E_\gamma) = \frac{\alpha + 1}{\alpha^2 + \alpha + 1} \tag{5}$$

where $\alpha = E_\gamma/m_ec^2$ and m_ec^2 is the electron rest mass energy. The values of C and D parameters for clover detector have been adopted from the study by Palit et al. [18] and are $C = (-9.9(7)) \times 10^{-5}$ keV^{-1}, $D = 0.446(6)$. The P values of the transitions of ^{63}Cu, following the present analysis, are plotted in Fig. 2. The plot also includes the corresponding theoretical values of P for pure transitions. The larger uncertainties on the Δ and the P values can be ascribed to the limited number of detectors at 90° along with the less than substantial yield of the nucleus. Such issues notwithstanding, the results of polarization analysis together with those of multipolarity measurements could be used to infer the multipole and the electric and magnetic nature of the gamma-ray transitions and assign spin-parities of the associated levels. These different procedures in the analysis exercise were applied for constructing the excitation scheme of ^{63}Cu nucleus and the results are elaborated in the subsequent section.
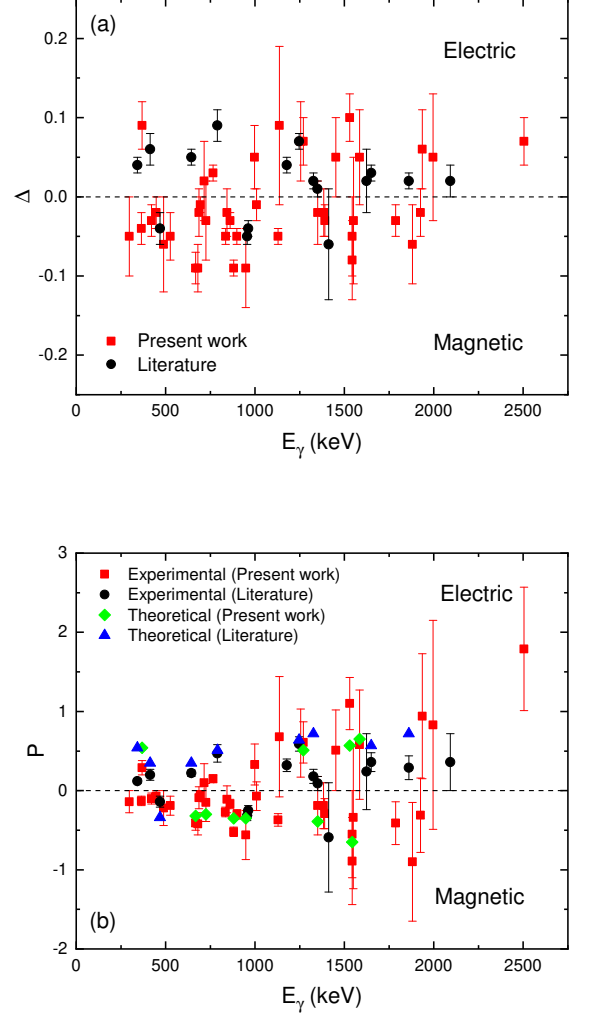
FIG. 2: (Color Online) (a) Polarization asymmetry (Δ) and (b) experimental and theoretical polarization (P) values, for different transitions of ^{63}Cu as observed in the present experiment. The theoretical polarization has been calculated for the pure stretched transitions only. The transitions for which electric and magnetic nature have been identified newly in this work are marked accordingly ("Present work") in the two figures. The electric and magnetic character of the other ("Literature") transitions were previously known and have been confirmed in the present work. Not all the previously known transitions have been included in these plots. All the Δ and P values, however, are recorded in Table I.
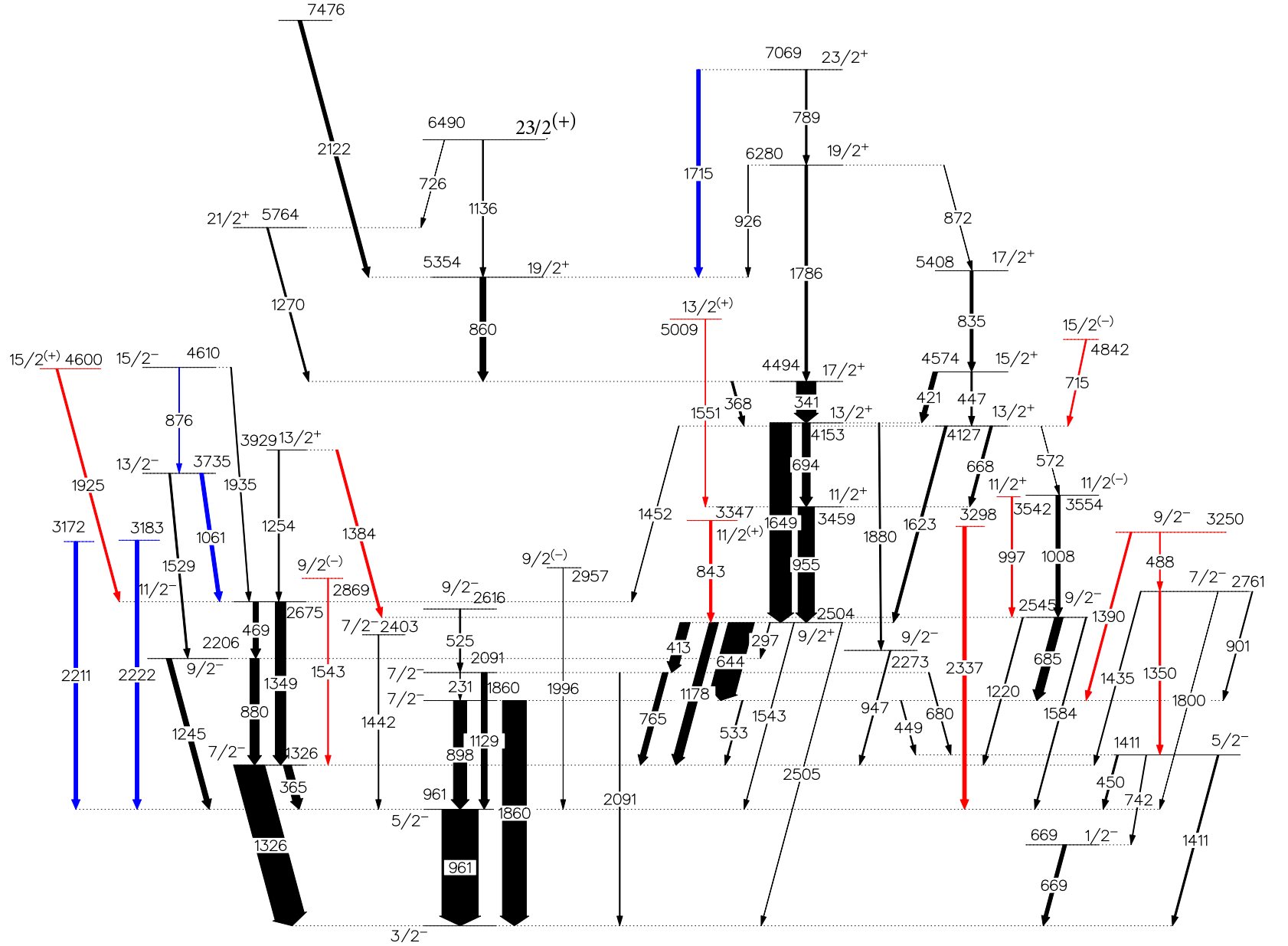
FIG. 3: (Color Online) Level scheme of ^{63}Cu, as resulting from the present work. The new transitions observed herein are marked in red. The previously known ones are from the work of Rai *et al.* [14]. The transitions represented through blue lines are tentative ones and weakly observed in the present study. Of these, the 876- and the 1715-keV were reported by Rai *et al.* [14] while the 1061, 2211, and 2222-keV are being newly proposed following the current investigation. The width of an arrow represents the intensity of the respective transition.

III.   RESULTS

The level scheme of the ^{63}Cu nucleus, as resulting from the present investigation, is illustrated in Fig. 3. The details of the γ-ray transitions, observed and studied in this work, along with the characteristics of the excited states are recorded in Table I. Following this work, 11 new γ-ray transitions have been placed in the level scheme of ^{63}Cu. In addition 3 γ-ray transitions have been tentatively identified for the nucleus and have accordingly been placed in the excitation scheme. The multipolarity and/or the polarization of some of the γ-ray transitions have been measured for the first time in this study. The energies of the γ-ray transitions have been extracted from the weighted average of their (centroid) energy values as observed in different gated spectra. The level energies, accordingly, have been assigned from the weighted average of their energies resulting from the energies of the connected (through transitions) states. Representative gated spectra, that illustrate the $\gamma - \gamma$ coincidences constituting the level scheme, are recorded in Figs. 4, 5, and 6. Fusion-evaporation reactions, characteristically, populate several residual nuclei and γ-ray transitions from nuclei other than ^{63}Cu, that appear as contaminant peaks in these gated spectra, have also been labelled along with the identity of the emitting nucleus. In the presence of such interfering peaks, several checks on the $(\gamma - \gamma)$ coincidence relationships have been carried out while assigning the newly observed γ-ray transitions to the nucleus of interest. Many of the γ-rays characterizing the nucleus were known from earlier studies [13, 14]. Newly observed transitions have been assigned to the nucleus based on their observed coincidence(s) with one or more of these previously known transitions. Wherever possible, double-γ gates have been applied on γ-γ-γ cube for confirming an observed coincidence. However, this experiment used one of the light-ion (^{7}Li) beams that are known to favorably populate non-yrast low-spin states. Thus most of the newly observed γ-rays emanate from cascades of lower multiplicities and, consequently, their counts in the γ-γ gated spectra were sparse.

In this study, the level scheme of ^{63}Cu has been confirmed upto an excitation energy of $\approx$ 7 MeV and spin $11\hbar$. The population of excited states, however, exhibits a steep decrease in the intensity above energy $\approx$ 4.5 MeV and spin $8\hbar$. An important output of the present analysis is the identification of the level at 3929-keV as the yrast $13/2^+$. This is based on the values of the R_{ADO} and the polarization asymmetry of the transitions, 1254- and 1384-keV, de-exciting the state. The state was first reported by Rai et al. [14], albeit with only a tentative spin-parity assignment of $13/2^-$. The assignment, however, was not validated with any measurement of multipolarity or electric and magnetic character of the 1254-keV gamma-ray, that was observed in the study (while the 1384-keV

transition has been a new observation in the present work). The identification of 3929-keV state as the yrast $13/2^+$ puts aside the proposition of Chiara et al. [3] on the anomalous energy of the level, deviant from the trend of the energies for this state across the odd-A Cu isotopes (Fig. 13 of Ref. [3]). The argument was based on the identification of the yrare $13/2^+$ as the yrast one that, as it follows from the current work, was a misplaced assignment. The yrast $13/2^+$, as confirmed in our analysis, does fit in the systematic variation of its energy with changing neutron number in the Cu isotopes.

The 3347-keV state, de-excited by the 843-keV transition, is newly identified in this study and has been assigned a spin-parity of $11/2^{(+)}$. The tentative nature of the parity assignment is owing to the large uncertainty on the polarization value of the (843-keV) transition. Nevertheless, this is a new candidate for the yrast $11/2^+$, following the present investigation.

It is worth commenting on the observation of 1350-keV transition as the most dominant branch de-exciting the 2761-keV level, following this investigation; the transitions of weaker branchings had been previously known [12]. It may be mentioned that this 2761-keV state was not reported by Rai et al. [14] or Mukherjee et al. [13], in their study of ^{63}Cu populated through heavy-ion induced reactions. The level and its de-exciting gamma-ray transitions, other than the 1350 keV, were reported [12] in the investigations using (n,n') reaction. These were carried out in experimental setups consisting of a single detector. The 1350-keV transition might have been missed out owing to the absence of gamma-gamma coincidence measurement in these studies, since there is another transition of overlapping energy de-exciting the 2675 keV state of the same nucleus. The latter state and the transition had been previously reported by Rai et al. and Mukherjee et al. as well as observed in studies using the (n,n') reaction.

It is imperative to put forth the arguments associated with definite multipolarity assignments for some of the γ-ray transitions, despite the considerable uncertainties on the their polarization values. The gamma-ray transitions 297.3, 685.3, 693.5, 1349.3, 1411.2, 1441.6, and 1623.1 keV are known from previous studies and connect levels that are of known spin-parities. These are respectively listed in the ENSDF [12] database, for the ^{63}Cu nucleus, as 297.0 ($E_i = 2505.08$ keV), 686.3 ($E_i = 2547.28$ keV), 694.3 ($E_i = 4155.56$ keV), 1350.1 ($E_i = 2676.84$ keV), 1412.08 ($E_i = 1412.16$ keV), 1442.7 ($E_i = 2404.66$ keV), and 1624.0 ($E_i = 4129.57$ keV) keV transitions, de-exciting the levels of energies indicated in the parentheses. For some of these, multipolarity and/or electric and magnetic assignments are also listed therein. In the light of the evaluated information on these gamma-rays, combined with the results of the ADO and the polarization measurements of the present

work, assignments have been made or confirmed herein. The 1451.8 keV gamma-ray has been reported by Rai *et al.* [14], without any multipolarity or electric and magnetic assignment, to connect previously known states (4129.57 and 2676.84 keV) that are included in the ENSDF database. The assignments have now been made for this transition while considering the established spin-parities of the associated states and the measurements of the present study. The transition 871.6 keV was first reported by Rai *et al.*, without any assignment of multipolarity or electric and magnetic nature. The ADO and the polarization value of the present analysis, even with the uncertainties included, implies a mixed M1+E2 nature. The spin-parities of the associated levels have been established from the measurements on other and more intense transitions. Similarly, the 1008.1 keV transition was first reported by Rai *et al.* without any assignments. The spin-parity of the initial level was indicated to be tentative therein. In the present analysis, the ADO and the polarization values, with the uncertainty included, are indicative of a M1 character. However, the same has been recorded as a tentative assignment, owing to the uncertainty on the polarization value, and, accordingly, the parity assignment of the initial level is also tentative. The transitions 715.1, 842.8, 1543.1, 1550.6, and 1924.5 keV have been identified as new ones in the present work. The identification of these transition give rise to new respective energy levels. However, owing to the uncertainties on the polarization values of these transitions, the assignments of their electric and magnetic nature and the parity of the de-excited levels have been recorded as only tentative. That notwithstanding, it may be noted that the ADO values of these transitions are reasonably conclusive towards their multipolarity assignments. Further, the 1995.8 keV transition was known from the previous studies and has been listed (as 1996.8 keV, de-exciting the level at 2957.29 keV) in the ENSDF database, without any multipolarity or electric and magnetic assignments. The latter have been made in the present study. It may also be noted that the other transitions that were identified [12] to be de-exciting the same level (2957.2 keV), along with the 1995.8 keV transition, could not be confirmed in the present work. The 1349.8 keV transition has been reported for the first time in the present work. The ADO value is that of a pure dipole while the result of the polarization analysis is not conclusive owing to the associated uncertainty. The polarization asymmetry of this transition had to be extracted from spectra corresponding to gate on transition that would not be in coincidence with the 1349.3 keV one, de-exciting the 2675 keV level. Consequently, the count statistics in the spectra for analyzing the polarization (of the new 1349.8 keV transition) was less than optimum and that led to increased uncertainty on the result. The latter is

thus used to quote a tentative assignment. However, the spin-parity of the initial (2761 keV) level has been established from the ADO and the polarization values of the 1799.6 keV gamma-ray, that is also de-exciting the state. Similarly, the 488.3 keV transition de-exciting the 3249.6 keV level has been identified as a new transition in this work. The spin-parity of the initial state has been fixed by a more intense (1389.8 keV) transition de-exciting the same level and with more definite assignment of multipolarity and electric and magnetic nature. The 996.6 keV transition has been identified as a new one de-exciting the 3542 keV level that is newly established in this study. The ADO and the polarization values for the transition indicate it to be of mixed E1+M2 character and the spin-parity of the de-exciting state has been assigned accordingly. The 2336.5 keV has been identified as a new transition that de-excites the 3297.9 keV state of the nucleus. However, the count statistics of this transition peak in the gated spectra is rather sparse for determination of R_{ADO} and polarization. The transitions 2211.0 and 2222.0 keV appear as a convoluted peak in the (961 keV) gated spectrum and could not be confirmed as individual transitions, in the absence of additional (possible) gates. These have thus been tentatively assigned to the excitation scheme of the ^{63}Cu nucleus.

It is interesting to note that there are a number of transitions in ^{63}Cu that have been assigned, tentatively or conclusively, to be of E1+M2, E2+M3 or M2+E3 nature, following this study. As far as these "rare assignments" are concerned, it may be mentioned that some of these (297.3, 1178.0, 1349.3, 1623.1 keV) were previously known while for some the spin-parities of the initial and/or the final states are known, more definitively, from the multipolarities and the electric and magnetic character of other transitions. The latter have either been observed in previous studies or in the present measurement. We may also mention that the higher multipolarities do not necessarily translate into long lifetimes as per the Weisskopf (single particle) estimates, at least with respect to the γ-γ coincidence window of ≈ 100 ns that is chosen for measurement. Even if they do, the branching of the corresponding γ-ray transition is measured to be sufficiently insignificant to impact the level lifetime.

The level structure of ^{63}Cu, as validated or established through the present investigation, is complex and irregular in character and indicates single particle excitations as the principal mechanism for generating low and medium spin states in this nucleus. The discussions hereafter pertain to interpreting the particle configurations associated with the states based on comparison with calculations in the shell model framework.

TABLE I: Details of the levels and the γ-ray transitions in ^{63}Cu observed in the present work. E_i and E_γ are respectively the energy of a state and the γ-ray transition(s) de-exciting it. I_γ is the intensity of the γ-ray transition. The uncertainty on I_γ include the statistical as well as the systematic contribution. The latter can be ascribed to the uncertainty on the efficiency calibration as well as uncertainty from the difference in the geometry of the experimental target and the radioactive source that was used for efficiency calibration. B.R. is the branching ratio of the transition. The B.R.s, if possible, have been extracted from gate on the transition(s) feeding the respective state. In case such a gate was not available, the B R.s were determined from the relative intensities of the transitions. J_i^π is the spin-parity of the state and J_f^π is that of the final level being fed by the transition. As described in the text, R_{ADO}, Δ and P are respectively the ADO value (Equation 1) of the transition, its polarization asymmetry (Equation 2) and its polarization (Equation 3) value. The new results (transitions, levels, multipolarities, electric and magnetic assignments) from this work have been indicated in **bold** font. The assignments not marked in bold font are confirmations of those derived from the previous measurements [14].

E_i (keV)	E_γ (keV)	I_γ	B.R.	J_i^π	J_f^π	R_{ADO}	Δ	P	Multipolarity
668.8(2)	668.8(2)		1.00	$1/2_1^-$	$3/2_1^-$				M1+E2^N
961.4(1)	961.4(1)	1000	1.00	$5/2_1^-$	$3/2_1^-$	0.69(2)	-0.04(1)	-0.25(6)	M1+E2
1326.0(1)	364.5(1)	219(5)	0.19(2)	$7/2_1^-$	$5/2_1^-$	0.65(2)	**-0.04(2)**	**-0.13(6)**	**M1+E2**
	1326.0(1)	828(17)	0.81(2)	$7/2_1^-$	$3/2_1^-$	1.33(2)	0.02(1)	0.18(9)	E2
1411.2(2)	449.6(3)	47(2)	0.41(4)	$5/2_2^-$	$5/2_1^-$	0.87(9)			D+Q
	741.8(5)	20(4)	0.18(4)	$5/2_2^-$	$1/2_1^-$				E2^N
	1411.2(1)	47(2)	0.41(4)	$5/2_2^-$	$3/2_1^-$	0.90(5)	-0.06(7)	-0.59(69)	(M1+E2)
1860.0(1)	448.8(5)	27(8)	0.02(2)	$7/2_2^-$	$5/2_2^-$	**0.63(5)**			**D+Q**
	533.2(5)	34(8)	0.03(2)	$7/2_2^-$	$7/2_1^-$	**1.04(26)**			**D+Q**
	898.2(1)	364(8)	0.34(2)	$7/2_2^-$	$5/2_1^-$	0.98(2)	-0.05(1)	-0.30(6)	M1+E2
	1860.4(1)	659(14)	0.61(2)	$7/2_2^-$	$3/2_1^-$	1.12(3)	0.02(1)	0.29(15)	E2
2090.8(1)	230.6(5)	15(3)	0.02(1)	$7/2_3^-$	$7/2_2^-$	**0.87(7)**			**D+Q**
	680.2(3)	27(3)	0.05(1)	$7/2_3^-$	$5/2_2^-$	**0.93(4)**	**-0.09(3)**	**-0.42(14)**	**M1+E2**
	764.7(1)	152(4)	0.37(1)	$7/2_3^-$	$7/2_1^-$	1.04(2)	**0.03(1)**	**0.15(5)**	**M1+E2**
	1129.4(1)	162(4)	0.49(1)	$7/2_3^-$	$5/2_1^-$	0.73(2)	**-0.05(1)**	**-0.37(8)**	**M1**
	2091.2(3)	23(3)	0.07(1)	$7/2_3^-$	$3/2_1^-$	**1.29(10)**	0.02(2)	0.36(36)	**(E2+M3)**
2206.1(1)	879.9(1)	251(6)	0.63(1)	$9/2_1^-$	$7/2_1^-$	0.80(4)	**-0.09(1)**	**-0.52(6)**	M1
	1245.1(1)	139(3)	0.37(1)	$9/2_1^-$	$5/2_1^-$	**1.11(17)**	0.07(1)	0.59(9)	**E2**
2273.3(2)	947.3(2)	32(1)	1.00	$9/2_2^-$	$7/2_1^-$	**0.92(9)**	**-0.09(5)**	**-0.56(31)**	**M1+E2**
2403.0(1)	1441.6(1)	19(1)	1.00	$7/2_4^-$	$5/2_1^-$	**0.73(6)**	**-0.01(6)**	**-0.10(61)**	**(M1)**
2504.0(1)	297.3(4)	24(1)	0.02(1)	$9/2_1^+$	$9/2_1^-$	1.04(6)	**-0.05(5)**	**-0.14(14)**	**(E1+M2)**
	413.1(1)	275(6)	0.22(1)	$9/2_1^+$	$7/2_3^-$	0.80(2)	0.06(2)	0.20(7)	E1
	644.1(1)	695(14)	0.55(1)	$9/2_1^+$	$7/2_2^-$	0.84(5)	0.05(1)	0.22(4)	E1
	1178.0(1)	243(5)	0.19(1)	$9/2_1^+$	$7/2_1^-$	0.99(4)	0.04(1)	0.32(8)	E1+M2
	1542.7(3)	14(1)	0.01(1)	$9/2_1^+$	$5/2_1^-$	1.27(6)	**-0.08(5)**	**-0.89(55)**	**M2**
	2504.7(2)	11(2)	0.01(1)	$9/2_1^+$	$3/2_1^-$	**1.00(5)**	0.07(3)	1.79(78)	**(E3)**
2545.4(1)	685.3(1)	231(5)	0.80(2)	$9/2_3^-$	$7/2_2^-$	0.99(5)	**-0.02(3)**	**-0.09(14)**	**(M1+E2)**
	1219.8(2)	30(2)	0.10(2)	$9/2_3^-$	$7/2_1^-$				
	1584.4(1)	30(1)	0.10(2)	$9/2_3^-$	$5/2_1^-$	**1.28(6)**	**0.05(6)**	**0.58(69)**	**(E2+M3)**
2615.9(2)	525.1(2)	35(2)	1.00	$\mathbf{9/2_4^-}$	$7/2_3^-$	**0.73(7)**	**-0.05(3)**	**-0.19(12)**	**M1**
2675.2(1)	468.7(1)	146(3)	0.33(3)	$11/2_1^-$	$9/2_1^-$	0.87(4)	-0.04(2)	-0.14(7)	M1
	1349.3(1)	288(6)	0.67(3)	$11/2_1^-$	$7/2_1^-$	1.34(3)	0.01(1)	0.09(9)	(E2+M3)
2761.0(2)	900.6(2)	25(3)	0.25(3)	$\mathbf{7/2_5^-}$	$7/2_2^-$	**0.99(8)**			**D+Q**
	1349.8(1)	**47(2)**	**0.47(3)**	$\mathbf{7/2_5^-}$	$5/2_2^-$	**0.87(3)**	**-0.02(4)**	**-0.19(37)**	**(M1)**
	1435.2(2)	22(1)	0.22(3)	$\mathbf{7/2_5^-}$	$7/2_1^-$	**0.63(6)**			**D+Q**
	1799.6(1)	5(1)	0.06(3)	$\mathbf{7/2_5^-}$	$5/2_1^-$	**0.72(7)**	**-0.07(6)**	**-0.98(84)**	**M1**
2869.1(3)	**1543.1(3)**	**25(1)**	**1.00**	$\mathbf{9/2_5^{(-)}}$	$7/2_1^-$	**0.74(7)**	**-0.05(5)**	**-0.55(55)**	**(M1)**
2957.2(5)	1995.8(5)	5(1)	1.00	$9/2_6^{(-)}$	$5/2_1^-$	**1.29(6)**	**0.05(8)**	**0.83(132)**	**(E2)**
3172.4(6)	**2211.0(6)**		**1.00**		$5/2_1^-$				
3183.4(9)	**2222.0(9)**		**1.00**		$5/2_1^-$				
3249.6(2)	**488.3(1)**	**22(1)**	**0.31(3)**	$\mathbf{9/2_7^-}$	$7/2_5^-$	**0.75(5)**	**-0.06(6)**	**-0.22(22)**	**(M1)**
	1389.8(1)	**49(2)**	**0.69(3)**	$\mathbf{9/2_7^-}$	$7/2_2^-$	**0.71(6)**	**-0.03(2)**	**-0.29(19)**	**M1**
3297.9(10)	**2336.5(10)**		**1.00**		$5/2_1^-$				
3346.8(2)	**842.8(2)**	**68(5)**	**1.00**	$\mathbf{11/2_1^{(+)}}$	$9/2_1^+$	**0.75(7)**	**-0.02(3)**	**-0.11(17)**	**(M1)**
3458.6(1)	954.6(1)	450(9)	1.00	$11/2_2^+$	$9/2_1^+$	0.66(2)	-0.05(1)	-0.32(6)	M1+E2
3542.0(2)	**996.6(2)**	**36(2)**	**1.00**	$\mathbf{11/2_3^+}$	$9/2_3^-$	**0.99(6)**	**0.05(4)**	**0.33(26)**	**E1+M2**
3553.5(2)	1008.1(2)	117(3)	1.00	$11/2_2^{(-)}$	$9/2_3^-$	**0.91(5)**	**-0.01(2)**	**-0.07(18)**	**(D+Q)**

Continued in next page

TABLE I – continued from previous page

E_i (keV)	E_γ (keV)	I_γ	BR	J_i^π	J_f^π	R_{ADO}	Δ	P	Multipolarity
3735.2(2)	1529.1(2)	47(1)		$13/2_1^-$	$9/2_1^-$	1.28(9)	0.10(3)	1.10(33)	E2
	1060.5(7)			$13/2_1^-$	$11/2_1^-$				
3929.4(2)	1254.1(1)	35(1)	0.36(2)	$13/2_1^+$	$11/2_1^-$	0.67(6)	0.07(5)	0.60(43)	E1+M2
	1384.3(2)	61(2)	0.64(2)	$13/2_1^+$	$9/2_3^-$	1.13(6)	-0.02(3)	-0.19(29)	M2+(E3)
4126.8(2)	572.5(6)	2(1)	0.04(1)	$13/2_2^+$	$11/2_2^{(-)}$	0.92(2)			D+Q
	667.7(1)	72(3)	0.40(1)	$13/2_2^+$	$11/2_2^+$	0.76(3)	-0.09(2)	-0.41(9)	M1
	1451.8(4)	14(1)	0.10(1)	$13/2_2^+$	$11/2_1^-$	0.97(17)	0.05(5)	0.51(51)	(E1+M2)
	1623.1(1)	71(3)	0.46(1)	$13/2_2^+$	$9/2_1^+$	1.08(1)	0.02(4)	0.24(48)	(E2+M3)
4152.9(1)	693.5(1)	216(5)	0.25(2)	$13/2_3^+$	$11/2_2^+$	0.73(2)	-0.01(1)	-0.05(5)	(M1)
	1648.9(1)	597(12)	0.71(2)	$13/2_3^+$	$9/2_1^+$	1.14(1)	0.03(1)	0.36(12)	E2
	1879.5(5)	37(1)	0.04(2)	$13/2_3^+$	$9/2_2^-$	1.10(9)	-0.06(5)	-0.90(75)	M2
4494.3(1)	341.4(1)	534(11)	0.88(2)	$17/2_1^+$	$13/2_3^+$	1.16(2)	0.04(1)	0.12(3)	E2
	367.6(3)	56(4)	0.12(2)	$17/2_1^+$	$13/2_2^+$	1.24(3)	0.09(3)	0.29(9)	E2
4573.5(2)	420.6(1)	125(4)	0.76(3)	$15/2_1^+$	$13/2_3^+$	0.93(4)	-0.03(2)	-0.10(7)	M1+E2
	447.2(2)	41(3)	0.24(3)	$15/2_1^+$	$13/2_2^+$	0.71(4)	-0.02(2)	-0.07(7)	(M1)
4599.7(2)	1924.5(2)	55(2)	1.00	$15/2_2^{(+)}$	$11/2_1^-$	1.12(6)	-0.02(3)	-0.31(47)	(M2,E2)
4610.4(3)	875.9(5)	13(5)	0.34(14)	$15/2_1^-$	$13/2_1^-$				
	1935.2(3)	25(1)	0.66(14)	$15/2_1^-$	$11/2_1^-$	1.20(8)	0.06(5)	0.94(79)	E2
4841.9(1)	715.1(1)	33(2)	1.00	$15/2_2^{(-)}$	$13/2_2^+$	0.70(4)	0.02(5)	0.10(24)	(E1)
5009.2(3)	1550.6(3)	15(1)	1.00	$13/2_4^{(+)}$	$11/2_2^+$	0.91(5)	-0.03(8)	-0.34(90)	(D+Q)
5354.0(1)	859.7(1)	162(5)	1.00	$19/2_1^+$	$17/2_1^+$	0.62(2)	-0.03(1)	-0.17(6)	M1+E2
5408.3(3)	834.8(2)	83(3)	1.00	$17/2_2^+$	$15/2_1^+$	0.69(2)	-0.05(1)	-0.27(6)	M1+E2
5763.9(1)	1269.6(1)	46(2)	1.00	$21/2_1^+$	$17/2_1^+$	1.28(7)	0.07(3)	0.61(26)	E2
6279.9(2)	871.6(2)	12(4)	0.14(4)	$19/2_2^+$	$17/2_2^+$	0.99(4)	-0.01(3)	-0.06(17)	(M1+E2)
	926.2(5)	10(1)	0.08(4)	$19/2_2^+$	$19/2_1^+$				
	1785.6(1)	76(3)	0.78(4)	$19/2_2^+$	$17/2_1^+$	0.63(5)	-0.03(2)	-0.41(27)	M1+E2
6489.7(2)	726.4(4)	3(1)	0.09(4)	$23/2_1^{(+)}$	$21/2_1^+$	0.82(8)	-0.03(5)	-0.15(24)	(M1+E2)
	1135.7(2)	29(1)	0.91(4)	$23/2_1^+$	$19/2_1^+$	1.07(7)	0.09(10)	0.68(76)	(E2)
7068.8(2)	788.9(1)	45(2)		$23/2_2^+$	$19/2_2^+$	1.17(7)	0.09(2)	0.47(11)	E2
	1715.3(5)			$23/2_2^+$	$19/2_1^+$				
7475.7(10)	2121.7(10)		1.00		$19/2_1^+$				

N Adopted from NNDC [12]

IV. DISCUSSIONS

Two different shell model calculations have been carried out in order to identify the single particle configurations underlying the level scheme observed in the present investigation. One of these considers the ^{63}Cu ($Z = 29, N = 34$) nucleus as a system of one valence proton and six valence neutrons outside the doubly-magic ^{56}Ni ($Z = 28, N = 28$) core. This calculation was implemented using the NuShellX@MSU [19] code. The model space consisted of $2p_{3/2}, 1f_{5/2}, 1p_{1/2}, 1g_{9/2}$ orbitals available for both protons and neutrons. The single particle energies are -9.8280 MeV for $2p_{3/2}$, -8.7087 MeV for $1f_{5/2}$, -7.8388 MeV for $1p_{1/2}$, and -6.261 MeV for $1g_{9/2}$ [14]. The valence nucleons were allowed an unrestricted occupation of the model space orbitals. The interaction chosen for the purpose was $jj44bpn$ [3], that is the pn version of the $jj44b$ interaction. The latter had been obtained through fitting binding energy and excitation energy data of nuclei with $Z = 28 - 30$ and $N = 48 - 50$ and thus includes data from Ni-isotopes in the process. The energies of the levels in ^{63}Cu and the corresponding particle occupancies resulting from the calculations using

the $jj44bpn$ interaction are recorded in Table II and Figs. 7 and 8. These also include the experimental level energies for comparison. In the model space defined for the $jj44bpn$ interaction, the dominant particle configurations underlying the negative parity states correspond to the odd proton and the six neutrons occupying $p_{3/2}, f_{5/2}$ and $p_{1/2}$ orbitals. The positive parity states are predominantly based on particle configurations of the type $\pi(f_{5/2}^{0-1} p_{3/2}^{0-1}) \otimes \nu(f_{5/2}^{1-3} p_{3/2}^{2-4} g_{9/2}^1)$. Most of the states are of considerably mixed configurations with maximum $\approx$ 10-15% probability, for the numerically dominant ones, and with competing contributions from other configurations.

This work was primarily aimed at understanding the particle configurations underlying the low- and medium-spin regime of ^{63}Cu, as an instance of single particle excitations characterizing the level structures of nuclei around the ^{56}Ni core. In this context, (proton) excitations across the $Z = 28$ shell closure have been identified to be of possible significance [3]. In order to probe the impact of such excitations in ^{63}Cu, an alternate calculation has been carried out in the shell

710
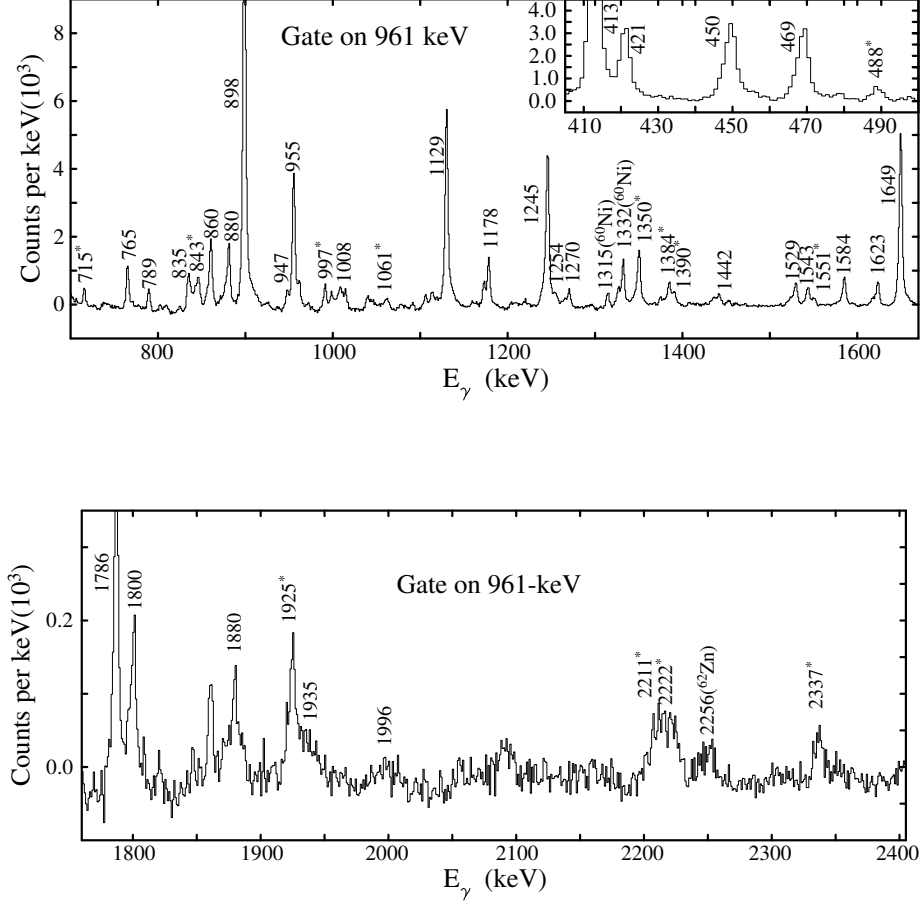
FIG. 4: Spectra projected from a γ-γ coincidence matrix with gate on 961-keV transition. The two spectra illustrate different energy ranges of the resulting projection. The new transitions assigned to ^{63}Cu are marked with *. The transition peaks observed due to other nuclei populated in the same reaction are labelled appropriately. The 488 keV transition, newly assigned to ^{63}Cu in this study, is illustrated in the inset of the upper panel. The 450 keV transition peak, labeled in the inset, combines peaks at 449.6, 448.8 and 447.2 keV that are listed in Table I.

model framework and using a model space that includes the $f_{7/2}$ orbital for protons in addition to the orbitals ($f5pg9$) used in the preceding calculations. The core is of ^{48}Ca ($Z = 20, N = 28$) wherein the neutron $f_{7/2}$ orbital is frozen with maximum occupancy. Excitations of upto two proton have been allowed from the $f_{7/2}$ to the $f_{5/2}p$ orbitals and upto two neutrons from the $f_{5/2}p$ orbitals to the $g_{9/2}$ orbital. The model space is hereafter referred to as the truncated $fpg9$. The pfg_{9a} interaction, originally reported by Sorlin et al. [7] and later modified by Srivastava [8], has been used for the purpose. Shell model code ANTOINE [20] was employed for this calculation. The results are presented in Table III and in Figs. 7 and 8. It may be noted that most configurations for the states have the $f_{7/2}$ orbital filled. The summed contributions of excitation from the $f_{7/2}$ orbital are included in the last column of Table III are

noted to be only of modest probabilities, that on average around 10% and, at most 17% for a few of them. It is possible that the configurations are indicative of a transitional behavior of particle excitations that may evolve, such as with respect to the $f_{7/2}$ occupancy, with changing valence nucleon number outside the ^{48}Ca core. The configurations in the truncated $fpg9$ model space that mostly contribute to the negative parity states are of the type $\pi(f_{7/2}^{8} p_{3/2}^{0-1} f_{5/2}^{0-1} p_{1/2}^{0-1}) \otimes \nu(p_{3/2}^{2-4} f_{5/2}^{1-4} p_{1/2}^{0-2})$. The positive parity levels exhibit, with few exceptions, large ($\approx$ 0.4 to 1.4 MeV) deviations between the experimental level energies and those calculated using the pfg_{9a} interaction. The particle occupancies constituting the positive parities correspond to the single proton in $f_{5/2}$ or $p_{3/2}$ orbital and one neutron in the $g_{9/2}$ orbital along with odd neutrons in one of the $f5p$ orbitals.
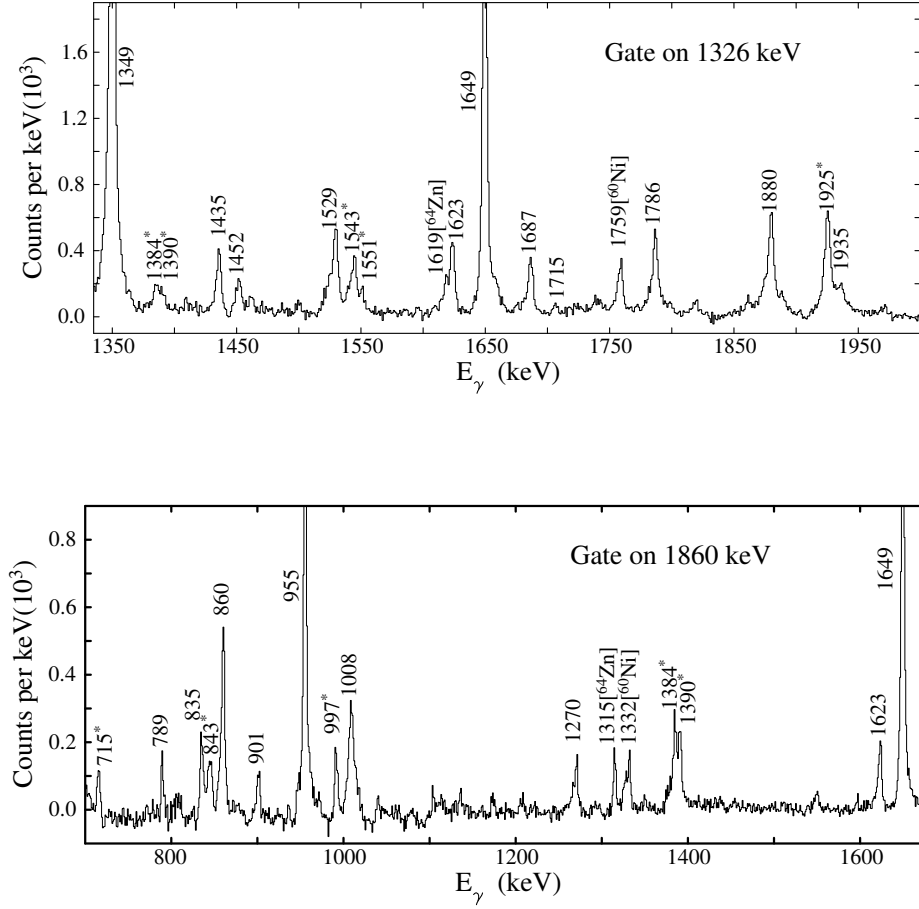
FIG. 5: Gated spectra extracted from the γ-γ coincidence matrix of the present data. The gated energies (1326 and 1860 keV) are indicated in the respective spectrum. The new transitions assigned to ^{63}Cu are marked with *. The transition peaks observed due to other nuclei populated in the same reaction are labelled appropriately. The 488 keV transition, newly assigned to ^{63}Cu in this study, has been observed in these spectra but not illustrated here.

These are similar to the configurations of the positive parity states in the $jj44bpn$ model space.

A discussion on the comparison between the experimental and the calculated level energies follows. The sequence of experimentally observed negative parity states is reproduced in the calculations with the $jj44bpn$ interaction. This is similar to the findings of Rai et al. [14] on this (^{63}Cu) nucleus, using the $jj44b$ interaction, and an improvement over the results obtained by Chiara et al. [3] on the neighbouring ^{65}Cu isotope wherein calculations using the $jj44b$ interaction did not quite reproduce the sequence of observed negative parity states. The present work compares the calculated negative parity states, with the experimental ones, for more number of levels of the same spin as well as upto levels of higher spins vis-a-vis that reported by Rai et al.

or Chiara et al.. This was with the objective to probe the efficacy of the shell model calculations for both yrast and non-yrast excitations. The comparison between the experimental and the calculated level energies is with respect to the levels that have been observed or confirmed in the present investigation. The (yrast) $5/2^-_1$ ($E_{exp} = 961\ keV$) and $7/2^-_1$ ($E_{exp} = 1326\ keV$) are well reproduced in the calculations using the $jj44bpn$ interaction. The calculated (yrare) state of $5/2^-_2$ ($E_{exp} = 1411\ keV$) different by ≈ 200 keV with the experimental one while $7/2^-_2$ ($E_{exp} = 1860\ keV$) exhibit deviation of ≈ 350 keV with respect to the experimental energy. The higher excited state of $7/2^-$, $7/2^-_3$ ($E_{exp} = 2091\ keV$), is also deviant by ≈ 200 keV. The configurations associated with the $5/2^-$ states are $\pi(p_{3/2}^{0-1}f_{5/2}^{0-1}) \otimes \nu(p_{3/2}^{2,3}f_{5/2}^{2,4}p_{1/2}^{0,1})$. Those for the $7/2^-$ states are $\pi(p_{3/2}^1) \otimes \nu(p_{3/2}^{3-4}f_{5/2}^{1-3}p_{1/2}^{0-1})$. Interestingly, the
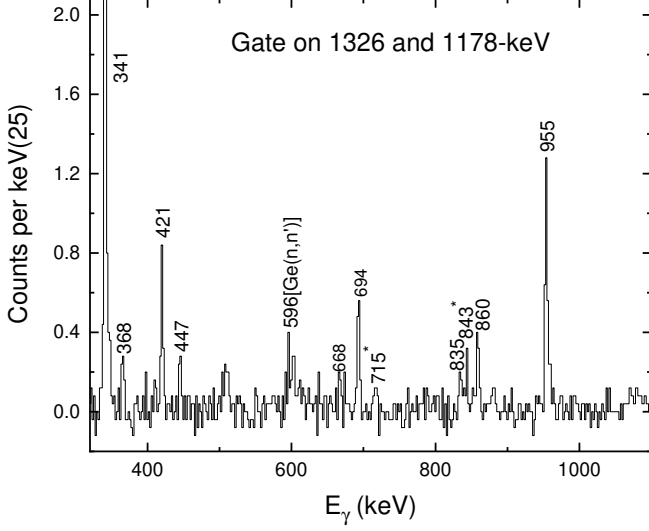
FIG. 6: Spectrum projected from the γ-γ-γ cube with double-γ gate applied on 1326- and 1178-keV transitions. The new transitions assigned to ^{63}Cu are marked with *. The sparse count statistics in the spectrum might not be quantitatively indicative of the relative intensities of the observed transitions.

FIG. 7: Comparison of the experimental level energies of negative parity states in ^{63}Cu with those calculated using the $jj44bpn$ and the pfg_{9a} interactions in the shell model framework.

configuration of the $3/2_1^-$ ground state has contribution from those corresponding to even number (mostly 2) of neutrons in the $g_{9/2}$ orbital. These configurations add up to $\approx 20\%$ of the total probability. Configurations based on such neutron occupancy of the $g_{9/2}$ orbital also contributes to the yrast and the yrare $5/2^-$ states and to varying extents, mostly summing upto $\approx 10\%$ of the probability, in the built of the other negative parity levels of ^{63}Cu. The $g_{9/2}$ orbital is a deformation driving one and occupancy of the same may impact the collectivity associated with the respective states. This may also indicate a transitional behaviour that underlie the evolving collectivity in the Cu isotopes.

The calculations using the pfg_{9a} Hamiltonian also reproduce the sequence of negative parity levels in ^{63}Cu. The overlap between the experimental and the calculated energies are within tens of keVs for the (yrast) $5/2_1^-$ ($E_{exp} = 961 \ keV$) as well as for the yrast $7/2_1^-$ ($E_{exp} = 1326 \ keV$) and the yrare $7/2_2^-$ ($E_{exp} = 1860 \ keV$) states. Such superior agreement between the calculated and the experimental energies is indicative of the role of $f_{7/2}$ orbital in the particle configurations that constitute these states. It is also worth noting that the pfg_{9a} calculated level energy of yrare $5/2_2^-$ ($E_{exp} = 1411 \ keV$) deviates from the experimental value by $\gtrsim 250$ keV and the corresponding particle configurations indicate visibly lesser contribution of the those based on $f_{7/2}$ excitations vis-a-vis their contribution in the yrast $5/2_1^-$ ($E_{exp} = 961 \ keV$) and

both the yrast $7/2_1^-$ ($E_{exp} = 1326 \ keV$) and the yrare $7/2_2^-$ ($E_{exp} = 1860 \ keV$). The leading configurations of the $5/2^-$ states in the truncated $fpg9$ model space are $\pi(f_{7/2}^8 p_{3/2}^{0-1} f_{5/2}^{0-1}) \otimes \nu(p_{3/2}^{3-4} f_{5/2}^2 p_{1/2}^{0-1})$. These are close to the calculated configurations in the $f5pg9$ model space and likewise largely mixed ones. The configurations for the $7/2^-$ states in the truncated $fpg9$ space are $\pi(f_{7/2}^8 p_{3/2}^1) \otimes \nu(p_{3/2}^3 f_{5/2}^2 p_{1/2}^1)$ that are close to those in the $f5pg9$ space. Interestingly, two levels of energies 3172- and 3183-keV (Fig. 3) could not be assigned spin-parity from the measurements within the present study. However, the calculations indicate levels with energies (3042 and 3192 keV) that are close to the aforementioned ones and of spin-parity $7/2^-$. This spin-parity of the levels would be in line with an experimental assignment of M1+E2 multipolarity for the (2211 and 2222 keV) transitions de-exciting them.

The calculated energy of the yrast $9/2_1^-$ ($E_{exp} = 2206 \ keV$) level, using the $jj44bpn$ interaction, is in reasonable compliance with the experimental value, by ≈ 150-keV, while the yrare ($E_{exp} = 2273 \ keV$) and the third excited state ($E_{exp} = 2545 \ keV$) of this spin-parity show up a difference of ≈ 300-350 keV with respect to the measured energies. The particle configurations of these $9/2^-$ states, in the $jj44bpn$ model space, are $\pi(p_{3/2}^{0-1} f_{5/2}^{0-1}) \otimes \nu(p_{3/2}^{2-4} f_{5/2}^{1-4} p_{1/2}^{1-2})$. As far as calculations with the pfg_{9a} Hamiltonian are concerned, the yrast $9/2_1^-$ ($E_{exp} = 2206 \ keV$) is well reproduced, within ≈ 100 keV, therein while the higher ones of

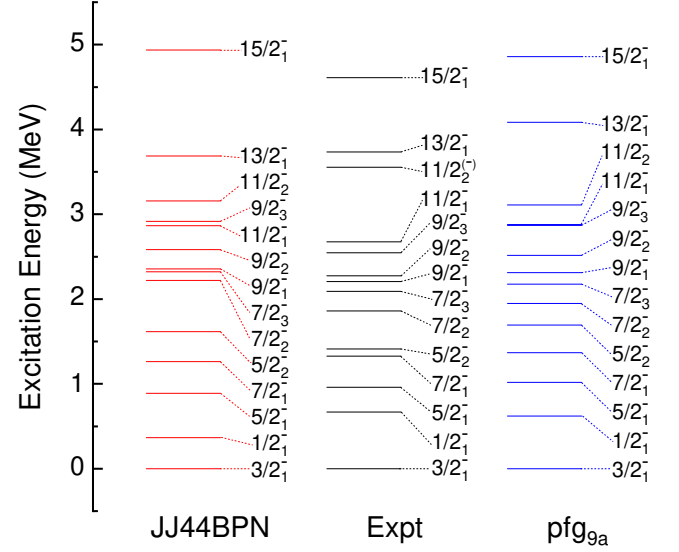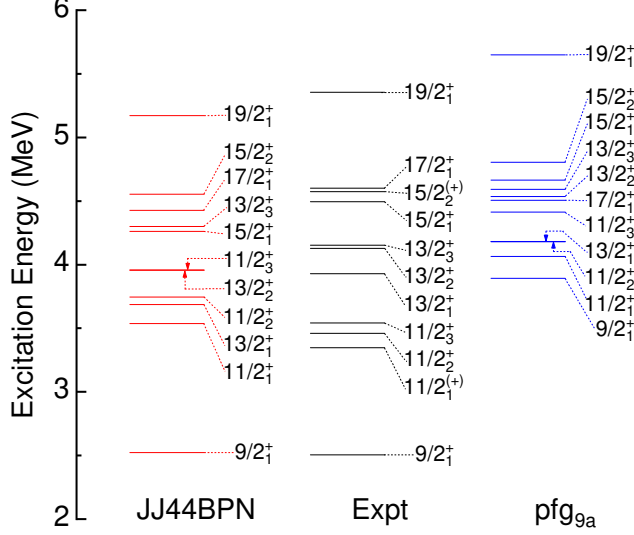FIG. 8: Comparison of the experimental level energies of positive parity states in ^{63}Cu with those calculated using the $jj44bpn$ and the pfg_{9a} interactions in the shell model framework.

this spin exhibit a difference of $\approx$ 250-300 keV with respect to their experimental values. It is noteworthy that the particle configurations underlying the $9/2^-$ states, as indicated by the pfg_{9a} calculations, include $\approx$ 10% - 17% contribution of those involving $f_{7/2}$ excitations. These are among the maximum contributions of such configurations as calculated for the states of ^{63}Cu.

The $11/2^-$ states exhibit similar overlap between the calculated and the experimental energies in calculations with the $jj44bpn$ and the pfg_{9a} Hamiltonians. The calculated energy of the yrast $11/2_1^-$ ($E_{exp} = 2675$ keV) is within $\approx$ 200 keV of the experimental value while the theoretical value of the yrare ($E_{exp} = 3553$ keV) one deviate by $\approx$ 400 keV from the measured energy. Similar (modest) compliance between the experimental level energy and that calculated with the two interactions, $jj44bpn$ and pfg_{9a}, is observed for the $13/2_1^-$ ($E_{exp} = 3735$ keV) state as well. In the $f5pg9$ space, the configurations of these states are $\pi(p_{3/2}^{0-1} f_{5/2}^{0-1}) \otimes \nu(p_{3/2}^{2-4} f_{5/2}^{2-4})$. The configurations in the truncated $fpg9$ space are calculated as $\pi(f_{7/2}^8 p_{3/2}^1) \otimes \nu(p_{3/2}^3 f_{5/2}^{1-2} p_{1/2}^{1-2})$. The $15/2_1^-$ ($E_{exp} = 4610$ keV) level energy is slightly better represented in the calculations with the pfg_{9a} interaction wherein the difference between the measured and the computed values is $\approx$ 250 keV while the same corresponding to the $jj44bpn$ Hamiltonian is $\approx$ 350 keV. The yrast negative parity states of higher spins, such as the $13/2_1^-$ ($E_{exp} = 3735$ keV) and the $15/2_1^-$ ($E_{exp} = 4610$ keV), have relatively pure configurations, both in the $jj44bpn$ as well as in the truncated $fpg9$

model space, particularly in the latter wherein the dominant configuration amounts to $\approx$ 50% of the relative probability.

The calculated level energies of the positive parity states using the $jj44bpn$ interaction are mostly of only modest agreement with the experimental values. This is similar to the findings of Rai et $al.$ in the context of the calculations using the $jj44b$ interaction. The lowest positive parity state, $9/2_1^+$ ($E_{exp} = 2504$ keV), exhibits excellent overlap between the calculated and the experimental energies. The particle configuration is largely mixed and of the type $\pi(p_{3/2}^{0-1} g_{9/2}^{0-1}) \otimes \nu(p_{3/2}^{1-4} f_{5/2}^{2-4} p_{1/2}^{0-2} g_{9/2}^{0-1})$. The theoretical level energies of the yrast $11/2_1^+$ ($E_{exp} = 3347$ keV) and the yrare $11/2_2^+$ ($E_{exp} = 3459$ keV) are deviant by $\approx$ 200-300 keV from the measured ones. The particle configurations of these states are severely mixed and correspond to one neutron occupancy of $g_{9/2}$ orbital along with an odd number of neutrons and the valence proton occupying the $f5p$ orbitals. The compliance between the theoretical and the experimental values of the other positive parity states is similar to the results of Rai et $al.$. For most of them, the agreement is only by $\approx$ 150-300 keV. The configurations are predominantly of a single neutron in the $g_{9/2}$ orbital along with an odd number of neutrons and the valence proton occupying the $f5p$ orbitals. The yrast $17/2_1^+$ ($E_{exp} = 4494$ keV), as an exception, has the calculated level energy within $\approx$ 70 keV of the experimental one. The state is also of more pure configuration, vis-a-vis other positive parity levels, and the dominant (particle) configuration, $\pi(p_{3/2}^1) \otimes \nu(p_{3/2}^4 f_{5/2}^1 g_{9/2}^1)$, is of a substantial $\approx$ 32% probability. It may also be noted that very few positive parity levels, such as the yrast $9/2_1^+$ ($E_{exp} = 2504$ keV) and the yrast $13/2_1^+$ ($E_{exp} = 3929$ keV), have somewhat noteworthy contribution from the configurations based on the valence proton occupancy of the $g_{9/2}$ orbital that sum upto $\approx$ 10-13% of the total probability. The latter are expected to assume significance with increasing neutron number, as has been reported by Chiara et $al.$ for ^{65}Cu nucleus. In the calculation with the pfg_{9a} Hamiltonian, most of the positive parity states are rather poorly (Table III, Fig. 8) represented. The exceptions are the yrast $13/2_1^+$ ($E_{exp} = 3929$ keV) state and the yrast $15/2_1^+$ ($E_{exp} = 4574$ keV) and the yrare $15/2_2^+$ ($E_{exp} = 4600$ keV) states, for which the overlap is in the range of $\approx$ 100-200 keV, and the yrast $17/2_1^+$ ($E_{exp} = 4494$ keV) state that has almost perfect overlap. However, the dominant particle configurations corresponding to these states do not manifest anything characteristic, to correlate with the superior agreement. These, for all positive parity states, are similar to the configurations in the $f5pg9$ model space and correspond to a single neutron in the $g_{9/2}$ orbital and five neutrons and the valence proton occupying the $f5p$ orbitals.

TABLE II: Energies of the levels of ^{63}Cu and the corresponding average particle occupancies of proton (p) and neutron (n) orbitals, as calculated in the shell model framework using the $jj44bpn$ Hamiltonian.

Expt (keV)	J^π	JJ44BPN (keV)		$f_{5/2}$	$p_{3/2}$	$p_{1/2}$	$g_{9/2}$
NEGATIVE PARITY STATES							
0	$3/2_1^-$	0	p	0.04	0.81	0.11	0.04
			n	2.35	2.57	0.59	0.49
669	$1/2_1^-$	367	p	0.13	0.43	0.41	0.03
			n	2.56	2.52	0.47	0.44
961	$5/2_1^-$	888	p	0.66	0.17	0.14	0.03
			n	2.69	2.30	0.47	0.54
1326	$7/2_1^-$	1264	p	0.03	0.83	0.10	0.04
			n	2.44	2.62	0.62	0.32
1411	$5/2_2^-$	1614	p	0.10	0.79	0.06	0.04
			n	2.27	2.54	0.81	0.38
1860	$7/2_2^-$	2219	p	0.08	0.81	0.06	0.04
			n	2.52	2.46	0.71	0.31
2091	$7/2_3^-$	2323	p	0.05	0.72	0.19	0.04
			n	2.66	2.58	0.50	0.25
2206	$9/2_1^-$	2356	p	0.77	0.09	0.11	0.03
			n	2.83	2.31	0.48	0.37
2273	$9/2_2^-$	2582	p	0.05	0.84	0.07	0.04
			n	2.23	2.76	0.71	0.29
2545	$9/2_3^-$	2916	p	0.08	0.81	0.07	0.04
			n	2.15	2.77	0.83	0.25
2675	$11/2_1^-$	2866	p	0.06	0.84	0.06	0.04
			n	2.38	2.73	0.62	0.28
3553	$11/2_2^{(-)}$	3156	p	0.07	0.86	0.03	0.03
			n	2.57	2.49	0.61	0.33
3735	$13/2_1^-$	3687	p	0.89	0.04	0.05	0.02
			n	2.87	2.34	0.49	0.31
4610	$15/2_1^-$	4937	p	0.05	0.92	0.01	0.02
			n	2.58	2.42	0.81	0.19
POSITIVE PARITY STATES							
2504	$9/2_1^+$	2523	p	0.07	0.42	0.05	0.47
			n	2.38	2.20	0.52	0.90
3347	$11/2_1^{(+)}$	3537	p	0.48	0.32	0.17	0.03
			n	2.35	2.02	0.44	1.20
3459	$11/2_2^+$	3746	p	0.10	0.58	0.13	0.19
			n	2.14	2.25	0.60	1.01
3542	$11/2_3^+$	3959	p	0.22	0.43	0.19	0.16
			n	2.27	2.15	0.58	1.00
3929	$13/2_1^+$	3687	p	0.08	0.56	0.10	0.27
			n	2.57	1.98	0.49	0.97
4127	$13/2_2^+$	3955	p	0.10	0.62	0.21	0.06
			n	1.71	2.69	0.48	1.11
4153	$13/2_3^+$	4301	p	0.52	0.23	0.21	0.04
			n	2.59	1.89	0.42	1.10
4494	$17/2_1^+$	4426	p	0.06	0.86	0.04	0.05
			n	1.38	2.83	0.66	1.14
4574	$15/2_1^+$	4261	p	0.61	0.18	0.19	0.02
			n	2.30	2.08	0.46	1.16
4600	$15/2_2^{(+)}$	4553	p	0.52	0.31	0.14	0.03
			n	2.28	2.16	0.43	1.13
5354	$19/2_1^+$	5171	p	0.93	0.03	0.04	0.01
			n	1.89	2.40	0.53	1.18

A more stringent test of the shell model calculations is the comparison between the calculated and the

experimental branching ratios. The latter are subject to the microscopic built of the states, as represented by the wavefunctions, and their overlap with the final states of the transitions. Theoretical branching ratios of few possible (M1, E2, M1+E2) transitions have been calculated in the present study and are compared to the corresponding experimental values in Table IV. This is probably the maiden instance when shell model calculated branching ratios are being compared with their experimental values for ^{63}Cu or even the neighboring isotopes. The missing entries for theoretical branching ratios imply that the respective transition is not predicted by the calculation. If the theoretical branching ratios of all transitions de-exciting a state do not add up to 100(%), it indicates that there are other transitions predicted by the calculations but the same have not been observed, either in this experiment or in any of the previous studies [13, 14] on the nucleus. The overlap between the calculated branchings, using the two interactions, and the experimental ones are rather mixed. It is noteworthy that the agreement between the calculated and the experimental values cannot be necessarily correlated with the overlap in the respective level energies. As far as the negative parity states are concerned, the only branching from yrast $5/2_1^-$ (E_{exp} = 961 keV) is reproduced by the two shell model calculations while the branchings from yrare $5/2_2^-$ (E_{exp} = 1411 keV) is better reproduced in the use of pfg_{9a} Hamiltonian. The calculations fall short of reproducing the experimental branchings from the $7/2^-$ states. It may be noted that the latter, as determined in this study, have also been verified to be in agreement with the values in the existing literature [12, 14]. The same validation has also been carried out for the branching ratios corresponding to the other states. The ratios of the transitions that de-excite the yrare $7/2_2^-$ (E_{exp} = 1860 keV) are different in the calculations with $jj44bpn$ and pfg_{9a}. However, none of these reproduce the comparable intensities of the 1860- and the 898-keV branches. Similarly, none of the calculations represent the comparable branching ratios of the 1129- and the 765-keV transitions de-exciting the $7/2_3^-$ state at 2091-keV. The ratios of the two branches from the yrast $9/2_1^-$ (E_{exp} = 2206 keV) come out (qualitatively) inverted in the calculations, albeit those using the pfg_{9a} Hamiltonian are somewhat nearer to the experimental values. The single branch de-exciting the yrare $9/2_2^-$ (E_{exp} = 2273 keV) is represented in the result from the pfg_{9a} interaction but not in the calculation with the $jj44bpn$. None of the calculations indicate the dominant branching of the 685-keV transition from the $9/2_3^-$ state at 2545-keV. The branchings from the yrast $11/2_1^-$ (E_{exp} = 2675 keV) state are well reproduced in the calculations using the pfg_{9a} interaction while the agreement is reasonable in that using the $jj44bpn$. The ratios of transitions de-exciting the yrast $13/2_1^-$ (E_{exp} = 3735 keV) state are faithfully represented in the calculations with the $jj44bpn$ interaction but

exhibit an inverted behavior in the truncated fpg framework. The pfg_{9a} calculated results for the yrast $15/2_1^-$ (E_{exp} = 4610 keV) state, however, are in excellent compliance with the experimental values. The overlap of the calculated level energies with the experimental values, for the positive parity states in ^{63}Cu, is rather modest for those using the $jj44bpn$ Hamiltonian and generally poor for the ones resulting from the pfg_{9a} interaction. Nevertheless, the single branches de-exciting the $11/2_{1,2}^+$ states at 3347- and 3459-keV or the yrast $19/2^+$ level are faithfully reproduced in the two shell model calculations. However, none of the calculations reproduce the comparable intensities of the 668- and the 1623-keV branches de-exciting the $13/2_2^+$ state at 4127-keV or the dominance of the 1649-keV branch of the $13/2_3^+$ state at 4153-keV. The dominant intensity of the 341-keV branch de-populating the yrast $17/2_1^+$ (E_{exp} = 4494 keV) state is well reproduced by the pfg_{9a} based calculations but not in those using $jj44bpn$. The ratios of the 447- and the 421-keV transitions, de-exciting the yrast $15/2_1^+$ (E_{exp} = 4574 keV) state, come out inverted from the use of pfg_{9a} interaction while these branches aren't reproduced in the calculations with the $jj44bpn$. The deviations in the calculated branching ratios might be the characteristic limitation of the shell model calculations for these nuclei around the shell closures at $N, Z = 28$. It is envisaged that additional data from level lifetime measurements, and the transition probabilities derived therefrom, would facilitate constraining the model calculations and lead to improved compliance between the experimental and the theoretical overlap of the states, manifested through the branching ratios and the transition probabilities. Sarantites *et al.* [21] had carried out spectroscopy and lifetime measurements in ^{61}Cu and had determined branching ratios and transitional probabilities therefrom. These were compared with the theoretical results of Castel *et al.* [22], for odd-A Cu isotopes, following their calculations in the framework of a model based on coupling of valence nucleons to the anharmonic vibrations of the even-even core. However, these were in the domain of low excitations and more comprehensive measurements are in order towards refinements in the (shell) model framework for improved representation of the experimental results.

The ^{63}Cu nucleus probably represents a transitional case of evolving significance of particle excitations from the $f_{7/2}$ orbital in the observed level structure of nuclei outside the ^{56}Ni core. The overlap between calculated and experimental level energies hasn't generally improved much, for the negative parity states, with the inclusion of the $f_{7/2}$ orbital in the model space and using the commensurate pfg_{9a} interaction. The yrare and the higher $7/2^-$ states are exceptions for which the compliance between the calculated and measured energies are visibly better (within $\approx$ tens of keVs) in the calculations with the pfg_{9a} interaction against those in the $f_{5/2}pg_{9/2}$

model space. While the dominant configurations emerging from the two calculations do differ in the particle occupancies of the $f_{5/2}, p_{3/2}$ and $p_{1/2}$ orbitals, the contribution of those based on proton excitations from the $f_{7/2}$ orbital remain modest in the truncated $fpg9$ space.

It would be worth pursuing the changing weightage of the latter through evolving (valence) nucleon number and consequent changes in the nucleon-nucleon interaction across the isotopic and the isotonic chains in this region.

TABLE III: Energies of the levels of ^{63}Cu and the corresponding average particle occupancies of proton (p) and neutron (n) orbitals, as calculated in the shell model framework using the $pfg9a$ Hamiltonian. The last column indicates, for the respective states, the summed contribution (in %) of the configurations corresponding to proton excitations from the $f_{7/2}$ orbital.

Expt (keV)	J^π	pfg_{9a} (keV)	$f_{7/2}$	$p_{3/2}$	$f_{5/2}$	$p_{1/2}$	$g_{9/2}$	$f_{7/2}^{6,7}p_{3/2}^{x}f_{5/2}^{y}p_{1/2}^{z}$ (Summed, %)
				Negative Parity States				
0	$3/2_1^-$	0	p 7.69	1.05	0.14	0.12	0.00	6.4
			n 8.00	2.88	2.08	0.93	0.11	
669	$1/2_1^-$	620	p 7.71	0.59	0.18	0.52	0.00	5.9
			n 8.00	2.92	2.30	0.66	0.11	
961	$5/2_1^-$	1017	p 7.62	1.11	0.17	0.10	0.00	16.6
			n 8.00	2.64	2.16	1.13	0.07	
1326	$7/2_1^-$	1366	p 7.66	1.09	0.14	0.12	0.00	11.0
			n 8.00	2.83	2.16	0.94	0.07	
1411	$5/2_2^-$	1693	p 7.69	0.50	0.44	0.37	0.00	3.7
			n 8.00	2.82	2.32	0.76	0.10	
1860	$7/2_2^-$	1947	p 7.66	1.07	0.14	0.14	0.00	11.0
			n 8.00	2.76	2.29	0.90	0.05	
2091	$7/2_3^-$	2176	p 7.62	0.98	0.14	0.26	0.00	11.4
			n 8.00	2.84	2.32	0.80	0.04	
2206	$9/2_1^-$	2313	p 7.67	1.09	0.13	0.11	0.00	9.8
			n 8.00	3.06	1.68	1.21	0.05	
2273	$9/2_2^-$	2515	p 7.58	1.10	0.15	0.16	0.00	17.2
			n 8.00	2.58	2.38	1.01	0.04	
2545	$9/2_3^-$	2867	p 7.66	1.01	0.14	0.19	0.00	11.2
			n 8.00	2.94	2.14	0.89	0.04	
2675	$11/2_1^-$	2879	p 7.69	1.09	0.12	0.09	0.00	6.9
			n 8.00	2.71	1.97	1.26	0.06	
3553	$11/2_2^{(-)}$	3111	p 7.64	1.11	0.14	0.10	0.00	11.3
			n 8.00	2.87	2.31	0.78	0.05	
3735	$13/2_1^-$	4083	p 7.68	1.10	0.14	0.09	0.00	15.5
			n 8.00	2.75	2.18	1.04	0.04	
4610	$15/2_1^-$	4859	p 7.70	1.10	0.13	0.07	0.00	12.5
			n 8.00	2.72	2.24	1.01	0.03	
				Positive Parity States				
2504	$9/2_1^+$	3892	p 7.78	0.76	0.16	0.30	0.00	11.0
			n 8.00	2.38	2.04	0.59	1.00	
3347	$11/2_1^{(+)}$	4065	p 7.79	0.77	0.17	0.28	0.00	11.8
			n 8.00	2.42	2.04	0.54	1.00	
3459	$11/2_2^+$	4179	p 7.76	0.74	0.20	0.29	0.00	13.9
			n 8.00	2.49	1.77	0.73	1.00	
3542	$11/2_3^+$	4412	p 7.78	0.83	0.17	0.22	0.00	11.5
			n 8.00	2.05	2.28	0.67	1.00	
3929	$13/2_1^+$	4182	p 7.77	0.90	0.13	0.20	0.00	12.9
			n 8.00	2.51	1.89	0.60	1.00	
4127	$13/2_2^+$	4536	p 7.79	0.68	0.28	0.26	0.00	10.2
			n 8.00	2.08	2.25	0.66	1.00	
4153	$13/2_3^+$	4591	p 7.78	0.70	0.27	0.25	0.00	10.4
			n 8.00	2.14	2.16	0.70	1.00	
				Continued in next page				

TABLEIII – continued from previous page

Expt (keV)	J^π	pfg_{9a} (keV)	$f_{7/2}$	$p_{3/2}$	$f_{5/2}$	$p_{1/2}$	$g_{9/2}$	$f_{7/2}^{6,7}p_{3/2}^x f_{5/2}^y p_{1/2}^z$ (Summed, %)
4494	$17/2_1^+$	4507	p 7.75	1.07	0.12	0.06	0.00	15.3
			n 8.00	2.60	1.34	1.06	1.00	
4574	$15/2_1^+$	4665	p 7.79	0.89	0.14	0.19	0.00	11.4
			n 8.00	2.29	2.03	0.68	1.00	
4600	$15/2_2^{(+)}$	4805	p 7.74	0.33	0.73	0.20	0.00	13.7
			n 8.00	2.36	1.99	0.66	1.00	
5354	$19/2_1^+$	5649	p 7.77	0.99	0.17	0.08	0.00	13.8
			n 8.00	2.48	1.57	0.95	1.00	

TABLE IV: Comparison of experimental Branching Ratio (B.R.) of the γ-ray transitions in ^{63}Cu with those resulting from two different shell model calculations used in this study. B.R.s are quoted in percentage and have been approximated to the nearest integer. The missing entries in the theoretical B.R.s represent that the respective calculation do not indicate such a transition. If the calculated B.R.s for a state do not add up to 100, it implies that the corresponding calculation indicate other transitions that have not been observed experimentally, either in the present work or in the previous studies [12, 14].

E_x EXPT	J_i^π	E_γ EXPT	B.R EXPT	E_x jj44bpn	B.R jj44bpn	E_x pfg_{9a}	B.R pfg_{9a}
				NEGATIVE PARITY			
961	$5/2_1^-$	961	100	888	100	1017	100
1326	$7/2_1^-$	365	19	1264	70	1366	74
		1326	81		30		26
1411	$5/2_2^-$	450	24	1614	8	1693	32
		1411	65		91		68
1860	$7/2_2^-$	1860	50	2219	2	1947	98
		898	45		23		<2
		533	2		9		>0
		449	3		65		>0
2091	$7/2_3^-$	2091	7	2324	1	2176	94
		1129	49		11		>6
		765	37		3		>0
		680	5		84		>0
		231	2		1		>0
2206	$9/2_1^-$	1245	37	2357	90	2313	72
		880	63		10		28
2273	$9/2_2^-$	947	100	2582	43	2515	100
2675	$11/2_1^-$	1349	67	2866	48	2879	59
		469	33		52		41
2545	$9/2_3^-$	1584	24	2916	1	2867	99
		1220	12		88		<1
		685	64		8		>0
3735	$13/2_1^-$	1529	<100	4055	98	4083	1
		1061	>0		2		99
4610	$15/2_1^-$	1935	66	4937	34	4859	64
		876	34		60		36

Continued in next page

TABLEIV – continued from previous page

E_x	J_i^π	E_γ	B.R	E_x	B.R	E_x	B.R
EXPT		EXPT	EXPT	jj44bpn	jj44bpn	pfg_{9a}	pfg_{9a}
				POSITIVE PARITY			
3347	$11/2_1^{(+)}$	843	100	3537	100	4065	100
3459	$11/2_2^+$	955	100	3746	98	4179	100
4127	$13/2_2^+$	668	40	3955	9	4536	99
		1623	46		14		1
4153	$13/2_3^+$	694	18	4301	1	4591	99
		1649	80		1		1
4494	$17/2_1^+$	368	12	4426	3	4507	
		341	88				100
4574	$15/2_1^+$	447	24	4261	2	4665	88
		421	76				12
5354	$19/2_1^+$	860	100	5171	2	5649	100

V. CONCLUSION

The low- and medium-spin excitations in the level structure of the ^{63}Cu nucleus have been investigated following their population in ^{59}Co(^{7}Li, $p2n$) reaction at E_{lab} = 22-24 MeV. 11 new transitions have been added to the existing level scheme. 3 new transitions have been tentatively placed therein. The spin-parity assignments have been made for the states from the angular correlation and the linear polarization measurements of the observed γ-rays. These measurements could be carried out for 10 (out of 11) new transitions. In addition, multipolarity assignments have been newly made or modified (with respect to the literature) for 29 transitions that were previously known for the nucleus. Similarly, electric and magnetic assignments have been newly made for 32 previously known transitions. The observed excitation scheme of the nucleus has been interpreted in the shell model framework through two different calculations. One of these was in the $f5pg9$ model space outside the ^{56}Ni core and using $jj44bpn$ interaction while the other was in the truncated $fpg9$ model space, for protons, outside the ^{48}Ca core and using the pfg_{9a} interaction. The objective of the latter was to probe the impact of proton excitations from the $f_{7/2}$ orbital in the level scheme of the nucleus and these have been identified to be of rather modest contribution in the built of the states of the nucleus, at least within the regime studied in the present endeavor. Branching ratios, of γ-ray transitions, were also calculated using the two interactions and compared with the experimental values. The overlaps have been mixed and not necessarily correlated with the agreement between the calculated and the experimental level energies. Further studies in the framework of the shell model, particularly on the influence of ^{56}Ni core broken configurations, are warranted and expected to facilitate the required refinements in the relevant interactions that are used for the calculations.

[1] R. F. Casten, *Nuclear Structure from a Simple Perspective* (Oxford University Press, 1999).

[2] W. A. Richter, S. Mkhize, and B. A. Brown, Phys. Rev. C **78**, 064302 (2008).

[3] C. Chiara, I. Stefanescu, W. B. Walters, S. Zhu, R. V. F. Janssens, M. P. Carpenter, R. Broda, B. Fornal, A. A. Hecht, N. Hoteling, et al., Phys. Rev. C **85**, 024309 (2012).

[4] D. A. Torres, F. Cristancho, L. L. Andersson, E. K. Johansson, D. Rudolph, C. Fahlander, J. Ekman, R. du Rietz, C. Andreoiu, M. P. Carpenter, et al., Phys. Rev. C **78**, 054318 (2008).

[5] M. Honma, T. Otsuka, T. Mizusaki, and M. Hjorth-Jensen, Phys. Rev. C **80**, 064323 (2009).

[6] S. Mukhopadhyay, B. P. Crider, B. A. Brown, S. F. Ashley, A. Chakraborty, A. Kumar, M. T. McEllistrem, E. E. Peters, F. M. Prados-Estévez, and S. W. Yates, Phys. Rev. C **95**, 014327 (2017).

[7] O. Sorlin, S. Leenhardt, C. Donzaud, J. Duprat, F. Azaiez, F. Nowacki, H. Grawe, Z. Dombrádi, F. Amorini, A. Astier, et al., Phys. Rev. Lett. **88**, 092501 (2002).

[8] P. C. Srivastava, Mod. Phys. Lett. A **27**, 1250061 (2012).

[9] P. Singh, R. Palit, D. Choudhury, P. C. Srivastava, S. Biswas, S. Saha, and J. Sethi, Eur. Phys. Jour. A **53**, 69 (2017).

[10] S. Samanta, S. Das, R. Bhattacharjee, S. Chatterjee, S. S. Ghugre, A. K. Sinha, U. Garg, Neelam, N. Kumar, P. Jones, et al., Phys. Rev. C **97**, 014319 (2018).

[11] S. Samanta, S. Das, R. Bhattacharjee, S. Chatterjee, S. S. Ghugre, A. K. Sinha, U. Garg, Neelam, N. Kumar, P. Jones, et al., Phys. Rev. C **99**, 014315 (2019).

[12] URL www.nndc.bnl.gov/ensdf/.

[13] B. Mukherjee, S. Muralithar, R. P. Singh, R. Kumar, K. Rani, , S. C. Pancholi, and R. K. Bhowmik, Pramana **55**, L471 (2000).

[14] S. Rai, B. Mukherjee, U. S. Ghosh, A. Biswas, A. Chakraborty, A. K. Mondal, S. Chakraborty, G. Mukherjee, I. Bala, S. Muralithar, et al., Eur. Phys. Jour. A **54**, 84 (2018).

[15] J. E. Koops and P. W. M. Glaudemans, Z. Phys. A **280**, 181 (1977).

[16] R. Palit, S. Saha, J. Sethi, T. Trivedi, S. Sharma, B. S. Naidu, S. Jadhav, R. Donthi, P. B. Chavan, H. Tan, et al., Nucl. Instr. Meth. Phys. Res. A **680**, 90 (2012).

[17] D. C. Radford, Nucl. Instr. Meth. Phys. Res. A **361**, 297 (1995).

[18] R. Palit, H. C. Jain, P. K. Joshi, S. Nagaraj, B. V. T. Rao, S. N. Chintalapudi, and S. S. Ghugre, Pramana **54**, 347 (2000).

[19] B. A. Brown and W. D. M. Rae, Nucl. Dat. Sheets **120**, 115 (2014).

[20] E. Caurier, G. Martnez-Pinedo, F. Nowacki, A. Poves, and A. P. Zuker, Rev. Mod. Phys. **77**, 427 (2005).

[21] D. G. Sarantites, J. H. Barker, N. H. Lu, E. J. Hoffman, and D. M. V. Patter, Phys. Rev. C **8**, 629 (1973).

[22] B. Castel, I. P. Johnstone, B. P. Singh, and K. W. C. Stewart, Can. Jour. Phys. **50**, 1630 (1972).